On-Chip NRZ-to-PRZ Format Conversion Using Narrow-Band Silicon Microring Resonator-Based Notch Filters

Linjie Zhou, Hui Chen, *Student Member, IEEE*, and Andrew W. Poon, *Member, IEEE*

***Abstract*—We report experimental demonstration and modeling of all-optical on-chip non-return-to-zero (NRZ) to pseudo-return-to-zero (PRZ) format conversion using narrow-band silicon microring resonator-based notch filters. Our proof-of-principle experiment using a carrier-injection-based tunable silicon microring resonator demonstrates NRZ-to-PRZ conversion at 3.6 Gbit/s. Our Fourier-transform-based modeling reveals in detail the format conversion dependence on the microring resonance Q factor, extinction ratio, phase response, and NRZ signal transition times, assuming signal format conversion of 40 Gbit/s.**

***Index Terms*—All-optical clock recovery, integrated optics, notch filters, optical resonators, optical signal processing, silicon photonics, waveguides.**

I. Introduction

SILICON microresonators with their key merits of compatibility with complementary metal–oxide–semiconductor (CMOS) microelectronics fabrication processes, narrow-band wavelength agility, micrometer-scale device footprint, and accessibility with integrated wire waveguides offer one of the building blocks for large-scale-integrated photonic circuits on a silicon chip. Recently, various optical signal-processing devices and circuits based on silicon microresonators have been proposed and demonstrated including multistage high-order microring-resonator add–drop filters [1], ultracompact optical buffers [2], carrier-dispersion-based modulators [3]–[6], and wavelength converters [7].

Previously, we proposed an all-optical on-chip non-return-to-zero (NRZ) to pseudo-return-to-zero (PRZ) format conversion using silicon second-order coupled-microring resonator-based notch filters [8]. Our approach potentially constitutes a highly integrated linear optics method to high-data-rate NRZ clock recovery on a silicon chip.

It is well known that NRZ-to-PRZ format conversion is essential for clock recovery from NRZ data format, which in principle carries no clock component. Conventional approaches to converting NRZ data format to PRZ data format (which carries a clock component) include using i) nonlinear semiconductor optics upon self-phase modulation in a semiconductor optical amplifier (SOA) [9]–[11] and ii) linear optics such as fiber Bragg grating (FBG)-based notch filters for suppressing the optical NRZ carrier frequency component [12], Fabry–Perot optical bandpass or comb filters for transmitting the weak clock components [13]–[16], and polarization-maintaining fibers [17]–[19] and integrated asymmetric Mach–Zehnder interferometer (AMZI) for generating relative delays [20]–[22].

However, nonlinear semiconductor optics methods impose high input signal power and slow operation speed limited by SOA carrier dynamics. Also an additional bandpass filter is needed in order to filter the frequency-chirped SOA signals to form the PRZ pulses, suggesting complicated designs and processes for on-chip integration. In contrast, linear optics approaches feature low complexity, and no active components are involved. Nonetheless, most conventional linear optics approaches are either fiber-based or based on bulk optical filters, and thus they are not readily applicable to on-chip optical signal processing. Although AMZI converters have been integrated on a silicon chip [22], the long AMZI arms needed to generate 10's ps relative delays between them still impose a relatively large device footprint.

In this paper, we detail our systematic experimental study and modeling of the proposed all-optical NRZ-to-PRZ format conversion using narrow-band silicon microring resonator-based notch filters. The rest of the paper is organized as follows. Section II briefly reviews the principle of using linear filtering for format conversion, Section III details our proof-of-principle experiment, Section IV presents the modeling and analysis, and Section V concludes this paper.

II. Principle

Fig. 1 illustrates the principle of all-optical NRZ-to-PRZ format conversion using a microring resonator-based notch filter. The concept is common to other linear optic filtering approaches to signal processing. Like the conventional FBG-based notch filter approach [12], the microring notch filter can suppress the optical NRZ carrier frequency component at the microring resonance and thereby effectively enhance the RF clock signal in the sidebands.

Fig. 1(a) illustrates the format conversion in time domain. An optical NRZ waveform is launched into the bus waveguide with the carrier wavelength λ_c at the microring notch filter center

Manuscript received September 14, 2007; revised November 2, 2007. Published August 29, 2008 (projected). This work was supported by the Research Grants Council of The Hong Kong Special Administrative Region, China, under Projects HKUST6112/03E and 618505.

L. Zhou was with the Department of Electronic and Computer Engineering, Hong Kong University of Science and Technology, Hong Kong SAR, China. He is now with the Department of Electrical and Computer Engineering, University of California at Davis, Davis, CA 95616 USA (e-mail: ljzhou@ucdavis.edu).

H. Chen and A. W. Poon are with the Department of Electronic and Computer Engineering, Hong Kong University of Science and Technology, Hong Kong SAR, China (e-mail: chenh@ust.hk; eeawpoon@ust.hk).

Color versions of one or more of the figures in this paper are available online at http://ieeexplore.ieee.org.

Digital Object Identifier 10.1109/JLT.2007.913742

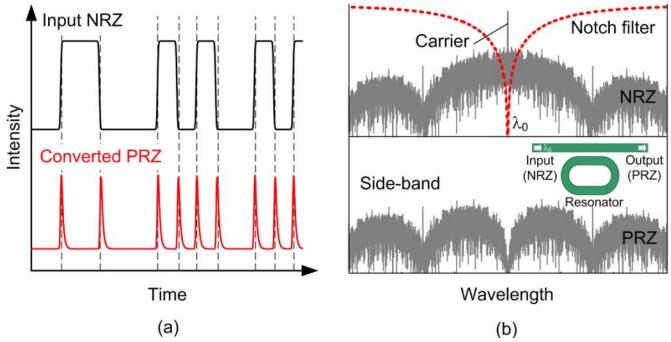

Fig. 1. Schematics of NRZ-to-PRZ format conversion using a microring resonator-based notch filter. (a) Schematic optical waveforms of the input NRZ signal and the converted PRZ signal at the NRZ signal transition edges. (b) Wavelength spectra of an input optical NRZ signal (top gray line), an ideal notch filter transmission (dotted line), and the converted PRZ signal (bottom gray line). The carrier wavelength λ_c of the input NRZ signal is at the microring notch filter resonance wavelength λ_o. Inset: schematic of the microring resonator notch filter.

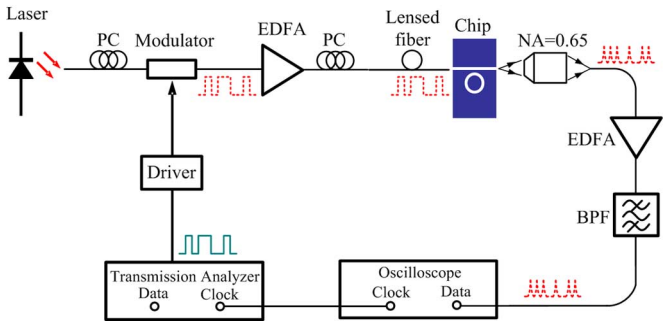

Fig. 2. Schematic experimental setup. PC: polarization controller; EDFA: erbium-doped fiber amplifier; BPF: bandpass filter.

wavelength λ_o. The resulting transmission yields PRZ pulses corresponding to the NRZ signal transition edges.

Fig. 1(b) depicts the notch-filter-based format conversion in spectral domain. The input optical NRZ signal contains a strong discrete carrier (λ_c) component with a broad side-band. After passing through a narrow-band notch filter with an ideal null transmission at λ_c, the carrier wavelength component is eliminated yet the sideband remains, which yields the converted PRZ pulses corresponding to the NRZ pulse transition edges. The inset depicts a schematic of the microring notch filter acting as an NRZ-to-PRZ format converter.

III. Proof-of-Principle Experiment

Fig. 2 shows schematically the experimental setup. A continuous-wave laser light (wavelength tunable from 1510 to 1580 nm) is modulated at a data rate of 3.6 Gbit/s (limited by the transmission analyzer). An erbium-doped fiber amplifier (EDFA) operated in saturation (~16 dBm saturation output power) is used to power-boost the modulated light before input-coupling to the bus waveguide through a polarization-maintaining single-mode lensed fiber. The device transmission is collected by an objective lens (NA= 0.65) and coupled into a single-mode fiber through another objective lens with NA = 0.1. The optical waveform, after another EDFA and a bandpass filter (3-nm bandwidth), is displayed by a 20-GHz-bandwidth oscilloscope. We tune the laser diode wavelength in order to characterize the signal transmissions both at off-resonance and on-resonance wavelengths of the microring notch filter. We also fine-tune the microring resonance wavelength by forward-biasing the p–i–n diode that is integrated into the microring and study the signal transmissions at different blue-shifted resonances.

A. Format Conversion Using a Tunable Microring Resonator

Fig. 3(a) shows an optical micrograph of our fabricated racetrack-shaped microring resonator-based notch filter on a silicon-on-insulator (SOI) substrate. We embed a lateral p–i–n diode around almost the entire microring in order to enable electrooptic resonance tuning using free-carrier plasma dispersion effect [23]. The device fabrication employs i-line photolithography, reactive ion dry etching, implantation, and aluminum (Al) sputtering (see [5]). The racetrack arc radius is 25 μm and the straight interaction length is 10 μm. The waveguide width is 0.4 μm and height is 0.21 μm with an etching depth of 0.18 μm. The coupling gap separation is 0.35μm. The p^+-doped (2×10^{19} cm^{-3}) and n^+-doped (1×10^{20} cm^{-3}) regions are positioned in the 30-nm-thick slab layer, with ~0.5–μm separations from the waveguide sidewalls in order to avoid excessive scattering and absorption losses due to mode-field overlapping with the highly doped regions.

Fig. 3(b) shows the measured TE-polarized (electric field in plane) transmission spectra of the microring notch filter with the p–i–n diode forward biased at 0, 1.0, 1.1, and 1.3 V. Upon 0-V bias, the transmission dip (Q ~ 9500) exhibits an extinction ratio (ER) of ~6 dB. As the diode is forward biased (beyond the threshold voltage of ~0.75 V), the resonance wavelength blue-shifts and the ER enhances with forward bias until reaching an optimum ER of ~16 dB (Q ~ 8000) upon a 1.1-V bias. This suggests a transition from overcoupling to critical coupling [24] as the carrier absorption increases. With further increment in forward biasing, however, the ER reduces, suggesting a transition from critical coupling to undercoupling.

Fig. 3(c)–(f) shows the measured 3.6-Gbit/s NRZ signal transmission waveforms at an off-resonance wavelength (0-V bias) and at on-resonance wavelengths upon forward biases at 0, 1.1, and 1.3 V. The off-resonance waveform largely follows the input NRZ signal. The optical signal displays a 10%–90% rise time of ~32 ps and a 90%–10% fall time of ~35 ps. In contrast, the on-resonance waveform upon 1.1-V bias displays PRZ pulses following the NRZ signal transition edges, with pulse widths of ~38 ps and a peak ER of ~4 dB. The on-resonance waveform upon 0-V (1.3-V) bias only displays a distorted NRZ signal, with an overshoot at the signal trailing (leading) edge and a dip at the signal leading (trailing) edge. The relatively low ERs upon 0- and 1.3-V biases render less optical carrier suppression, and thereby significant transmissions at the NRZ digital "1" levels and less pronounced PRZ pulses. We attribute the noise fluctuations observed in all the waveforms to amplified spontaneous emission noise from the two EDFAs.

B. Discussion

Our typical device insertion loss is ~20 dB (relative to the lensed fiber transmission intensity) for TE polarization, which we attribute to excessive fiber-to-waveguide coupling loss and

waveguide propagation loss. We estimate the fiber-to-waveguide coupling loss is ~13.5 dB originated from end-face reflection (~1.5 dB) and mode-mismatch losses (~12 dB). In general, fiber-to-waveguide coupling loss can be mitigated using three-dimensional or inverted adiabatic tapers [25], [26]. We measure the waveguide propagation loss to be ~20 dB/cm by using a cutback method. We attribute the waveguide propagation loss mainly to sidewall roughness-induced scattering, as our photolithography (i-line, 365 nm) and dry etching are not favorable for fabricating smooth sidewalls. In principle, the waveguide propagation loss can be reduced to 1–2 dB/cm [2] by minimizing sidewall roughness using e-beam lithography or CMOS-compatible deep-ultraviolet photolithography and optimized dry-etching processes. We note that we can only measure the TE polarization response of our device. For TM polarization, we measure no transmission, possibly due to excessive propagation loss, as the vertically polarized mode field is not well confined in the 0.21-μm-height waveguide core. This monopolarization response potentially imposes limitations for practical applications of our device in fiber networks, and it is likely that additional polarization splitters and converters are needed.

The resonance Q-factors in our devices are mainly limited by the waveguide sidewall roughness induced cavity loss. With improved fabrication technology, high-Q resonances up to 10^5 and beyond in microring resonators are possible [27].

In order to enhance the NRZ-to-PRZ format conversion, high-order notch filters with enhanced ERs and sharpened rolloffs can be used in favor of narrow-band filtering. Such high-order notch filter can be composed of series-coupled double microring resonators, as reported previously by our group [8]. Our experimental results revealed converted PRZ waveform at 3.6 Gbit/s with pulse widths of ~40 ps (48 ps) and pulse ERs of ~8 dB (6 dB) corresponding to the NRZ signal leading (trailing) edges by using a series-coupled microring notch filter with a Q-factor of ~14 000 and an ER of ~12 dB.

The carrier-injection-based electrooptic tuning adopted here has its own drawbacks. As carrier absorption always accompanies carrier dispersion, the resonance linewidth becomes broadened upon high carrier injection [see Fig. 3(b)] and thus practically limits the resonance wavelength tuning range to ~1 nm. Moreover, the resonance Q and ER inevitably vary with resonance wavelength blue-shift upon carrier injection. Thus, it imposes difficulties in differential tuning of series coupled microring resonators, in which identical resonance response for each microring resonator is needed in order to attain good high-order filtering performances.

In order to enable a wide resonance wavelength tuning range for channel selection or to compensate for the fabrication-induced stochastic variations in microring resonance wavelength, we can adopt other tuning mechanisms such as thermooptic tuning [28] or electrooptic tuning using liquid crystal as an upper cladding layer [29]. We note that both thermooptic-based and liquid crystal-based tuning does not impose excess loss for a wide range of wavelength tuning.

IV. Model

Here, we present a Fourier-transform-based model for NRZ-to-PRZ conversion [12] using a narrow-band microring resonator-based notch filter. For simplicity, we only model single-order microring resonator-based notch filters. We examine in detail the format conversion dependence on the microring resonance Q-factor, ER, phase response, and NRZ signal transition times.

We consider an N-bit pseudorandom bit sequence (PRBS) intensity waveform $\mathrm{b_i(t)}$ as the input NRZ data signal of levels "1" and "0." We express the electric field of the NRZ-modulated optical signal as

$$\mathrm{E_i(t)} = \mathrm{A_0}\sqrt{\mathrm{b_i(t)}}\exp(i\omega_c t) \tag{1}$$

where ω_c is the carrier frequency and A_0 is the signal field amplitude. We expand the modulated field envelope $\mathrm{A_0}\sqrt{\mathrm{b_i(t)}}$ as a Fourier series as follows:

$$A_0\sqrt{\mathrm{b_i(t)}} = A_0 \sum_{n=0,\pm1,\pm2,\ldots} a_n \exp(in\omega_0 t) \tag{2}$$

where $\omega_0 = 2\pi NT$ is the base frequency (T is the bit duration) and a_n is the Fourier coefficient of the nth harmonic component ($n = 0$ for the dc component) of the modulation envelope. We remark that a_n is determined by the NRZ signal rise-and-fall times.

We express the electric-field transmission for a single-order microring notch filter as [24]

$$\mathrm{T}(\omega) = \frac{\tau - \alpha\exp(in_{\mathrm{eff}}L\omega/c)}{1-\tau\alpha\exp(in_{\mathrm{eff}}L\omega/c)} \tag{3}$$

where τ is the waveguide field transmission coefficient through the waveguide-microring coupler ($\tau^2+\kappa^2=1$ for lossless coupling, where κ is the coupling coefficient), α is the round-trip cavity field loss factor ($\alpha = 1$ for an ideal lossless transmission), n_{eff} is the effective refractive index of the microring and the waveguide, L is the microring resonator round-trip length, c is the speed of light in free space, and ω is the light frequency. At resonance wavelength λ_{res}, we have $n_{\mathrm{eff}}L = m\lambda_{\mathrm{res}}$, where $m = 1, 2, 3, \ldots$.

Hence, the NRZ signal transmission through the microring notch filter yields

$$\mathrm{E_o(t)} = \mathrm{A_0} \sum_{n=0,\pm1,\pm2,\ldots} a_n T(\omega_c + n\omega_0) \times \exp[i(\omega_c + n\omega_0)t] \tag{4}$$

and we express the normalized output bit sequence intensity waveform as

$$\mathrm{b_o(t)} = \left|\frac{\mathrm{E_o(t)}}{A_0}\right|^2. \tag{5}$$

A. Resonance Q-Factor Dependence

Here, we examine the NRZ-to-PRZ format conversion at 40 Gbit/s using the model. We first consider three notch filters with different resonance Q-factors of 2×10^3 (3-dB linewidth of ~0.78 nm), 4×10^3(~0.39 nm), and 8×10^3(~0.19 nm), all

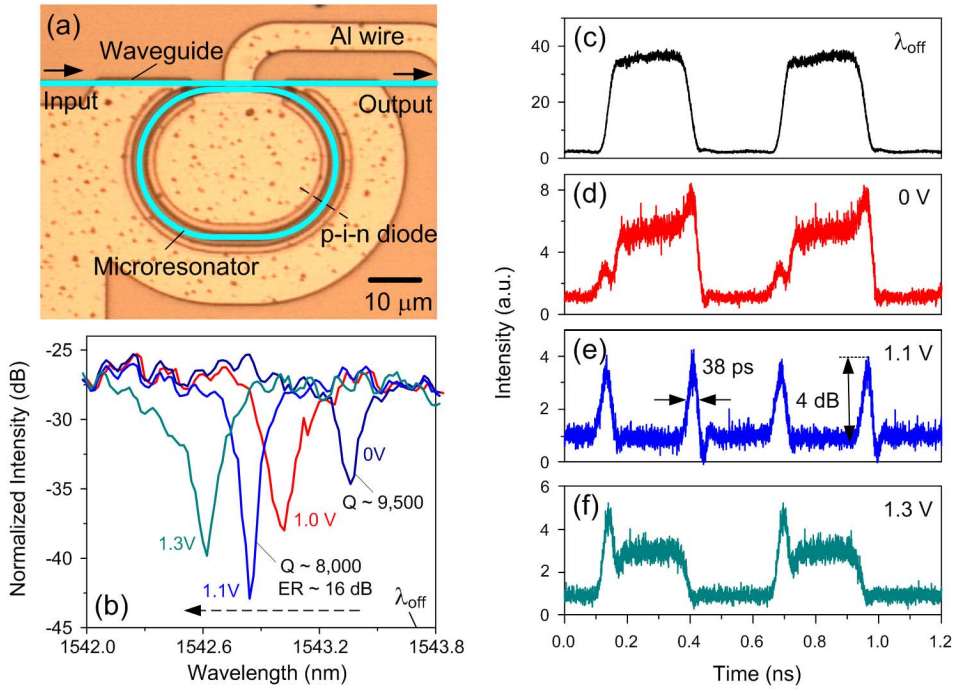

Fig. 3. (a) Optical micrograph of an electrically tunable racetrack-shaped microring resonator-based notch filter with laterally integrated p–i–n diode on an SOI substrate. (b) Measured TE-polarized throughput-port transmission spectra of the notch filter upon various forward-bias voltages. (c)–(f) Measured transmissions of a 3.6-Gbit/s NRZ waveform at (c) an off-resonance carrier wavelength λ_{off} ($\sim$1543.7 nm), (d) an on-resonance carrier wavelength upon 0-V forward bias ($\sim$1543.3 nm), (e) an on-resonance carrier wavelength upon 1.1-V forward bias ($\sim$1542.8 nm), and (f) an on-resonance carrier wavelength upon 1.3-V forward bias ($\sim$1542.6 nm).

with ER of 20 dB. The microring and the waveguide are assumed undercoupled ($\tau > \alpha$). We set the input NRZ signal carrier wavelength λ_c at the notch filter resonance wavelength λ_o.

Fig. 4 depicts a single-input NRZ waveform and the converted PRZ pulses after processing by these notch filters [using (5)]. The input NRZ waveform assumes a data rate of 40 Gbit/s with typical symmetrical rise and fall times of 6 ps. Our modeling shows PRZ pulses appearing at the leading and trailing edges of the NRZ signal, with higher pulse height at the leading edge (to be explained in the following section). As expected, the PRZ pulses' height and width depend on the resonance Q-factor. A high-Q (narrow-band) notch filter transmits more sideband frequency components and results in more pronounced PRZ pulses (higher in pulse height and wider in pulse width). With $\text{Q} = 2 \times 10^3$, the converted PRZ pulse height is only $\sim$0.13 normalized to the input NRZ pulse height and the PRZ pulse width is $\sim$5.5 ps. With $\text{Q} = 8 \times 10^3$, the PRZ pulse height becomes $\sim$0.5 normalized to the input NRZ pulse height and the PRZ pulse width is also broadened to $\sim$10 ps.

Nonetheless, we caution that a cavity Q of 8×10^3 suggests a 1/e cavity photon lifetime of $\text{Q}/\omega \approx 7$ ps, which yields wide enough PRZ pulses that can cause pulse overlap and interference within a single NRZ bit duration. Therefore, in order to avoid PRZ pulses overlap and interference, we can adopt notch filters with $\text{Q} < 8 \times 10^3$ for NRZ-to-PRZ conversion at data rate of 40 Gbit/s.

B. Resonance ER and Phase Response Dependences

Both the resonance ER and phase response affect the converted PRZ signal. Fig. 5(a)–(c) shows the microring notch filter transmission intensity (solid line) and phase (dotted line) responses [using (3)], assuming undercoupling with an ER of 10 dB [Fig. 5(a)], undercoupling with an ER of 20 dB [Fig. 5(b)], and overcoupling with an ER of 20 dB [Fig. 5(c)]. The Q-factors are 4×10^3 for all cases. We assume an input 40-Gbit/s NRZ waveform with rise and fall times of 6 ps, as shown in Fig. 5(d).

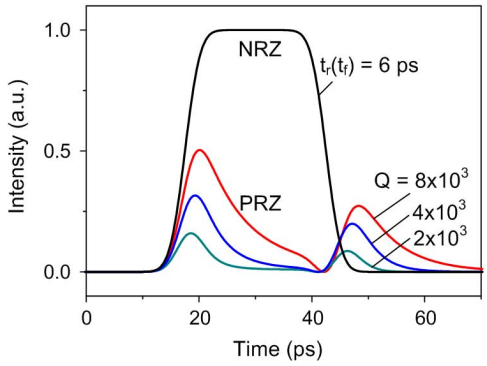

Fig. 4. Input 40-Gbit/s NRZ waveform with 6-ps rise and fall times and converted PRZ pulses after notch filters of $\text{Q} = 2 \times 10^3$, $\text{Q} = 4 \times 10^3$, and $\text{Q} = 8 \times 10^3$. All notch filters assume an ER of 20 dB.

Fig. 5(e) shows the PRZ pulses from the 10-dB notch filter. The relatively weak optical carrier suppression renders significant background transmission at the NRZ high level, resulting in a widened PRZ pulse at the NRZ leading edge with significant pulse overlap and interference with the PRZ pulse at the NRZ trailing edge.

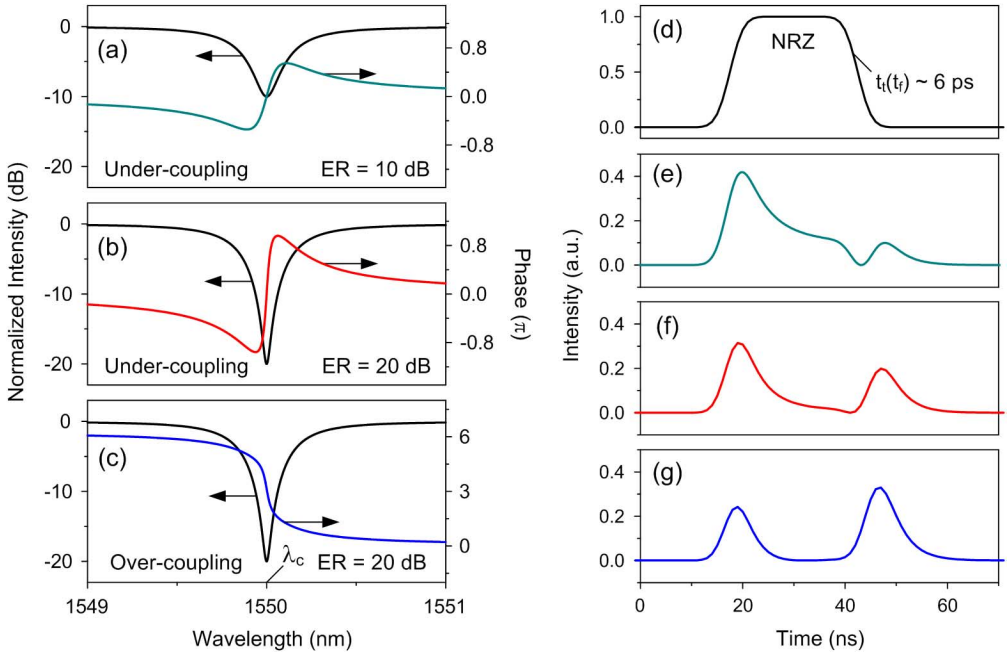

Fig. 5. (a)–(c) Notch filter transmission intensity (solid line) and phase response (dotted line) in (a) undercoupling regime with ER of 10 dB, (b) undercoupling regime with ER of 20 dB, and (c) overcoupling regime with ER of 20 dB. (d) Input 40-Gbit/s NRZ waveform with 6-ps rise and fall times. (e)–(g) Converted PRZ pulses after notch filters with corresponding transmission performances shown in (a), (b), and (c), respectively.

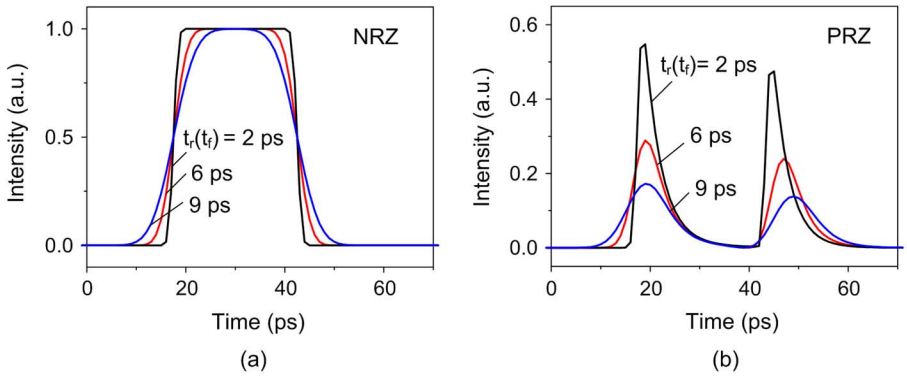

Fig. 6. (a) Input NRZ waveforms at 40-Gbit/s with rise (t_r) and fall (t_f) times of 2, 6, and 9 ps. (b) Converted PRZ pulses after a notch filter with $Q = 4 \times 10^3$ and ER of 20 dB.

Comparing undercoupling and overcoupling cases with the same ER (of 20 dB), we find that although the notch filter transmission intensity responses are identical, the phase responses are distinct. The different phase responses thus yield different converted PRZ signals, as shown in Fig. 5(f) and (g). In case the notch filter is in an undercoupling regime, the converted PRZ signal displays a strong pulse at the leading edge, yet in overcoupling regime, the strong pulse appears at the trailing edge, which is consistent with our experimental observations [see Fig. 3(d) and (f)].

C. NRZ Signal Transition Time Dependence

Fig. 6(a) and (b) shows three input 40-Gbit/s NRZ waveforms with rise and fall times of 2, 6, and 9 ps and the corresponding converted PRZ pulses. We assume a notch filter with ER of 20 dB and $Q = 4 \times 10^3$. As expected, with the shortest NRZ pulse transition times of 2 ps, the converted PRZ pulses display the highest pulse height of ~0.55 normalized to the input NRZ signal and the narrowest pulse width of ~4.3 ps. With the NRZ pulse transition times lengthened to 9 ps, the PRZ pulse normalized peak height drops to ~0.17, with pulse width broadens to ~10 ps. PRZ signals with a narrow pulse width and a large pulse height favor clock recovery [22].

V. Conclusion

We have experimentally demonstrated and modeled the proposed all-optical NRZ-to-PRZ format conversion using silicon electrooptically reconfigurable microring resonator-based notch filters. Our proof-of-principle experiments have shown that a single-order microring notch filter can convert a 3.6-Gbit/s input NRZ data signal to a PRZ signal with a pulse width of ~38 ps and an extinction ratio of ~4 dB. The choice of data rate here is only limited by our transmission analyzer data rate. We observed that the converted PRZ data quality highly depends on the microring notch filter extinction ratio and the waveguide-to-microring coupling regime. We have also developed a Fourier-

transform-based model that reveals in detail the format conversion dependence on several key parameters including the resonance Q-factor, the extinction ratio, the waveguide-to-microring coupling regimes, and the input NRZ signal transition times at 40-Gbit/s data rate. We therefore conclude that silicon microring resonator-based notch filters can act as all-optical on-chip NRZ-to-PRZ format converters, which can be relevant to high-data-rate NRZ clock recovery for optical communications network applications.

REFERENCES

[1] M. A. Popović, T. Barwicz, M. R. Watts, P. T. Rakich, L. Socci, E. P. Ippen, F. X. Kärtner, and H. I. Smith, "Multistage high-order microring-resonator add-drop filters," *Opt. Lett.*, vol. 31, no. 5, pp. 2571–2573, May 2006.

[2] F. Xia, L. Sekaric, and Y. Vlasov, "Ultracompact optical buffers on a silicon chip," *Nature Photon.*, vol. 1, pp. 65–71, Jan. 2007.

[3] C. A. Barrios, V. R. Almeida, R. Panepucci, and M. Lipson, "Electrooptic modulation of silicon-on-insulator submicrometer-size waveguide devices," *J. Lightw. Technol*, vol. 21, pp. 2332–2339, Oct. 2003.

[4] Q. Xu, B. Schmidt, S. Pradhan, and M. Lipson, "Micrometre-scale silicon electro-optic modulator," *Nature*, vol. 435, no. 7040, pp. 325–327, 2005.

[5] L. Zhou and A. W. Poon, "Silicon electro-optic modulators using p–i–n diodes embedded 10-micron-diameter microdisk resonators," *Opt. Expr.*, vol. 14, no. 15, pp. 6851–6857, Jul. 2006.

[6] Q. Xu, S. Manipatruni, B. Schmidt, J. Shakya, and M. Lipson, "12.5 Gbit/s carrier-injection-based silicon micro-ring silicon modulators," *Opt. Expr.*, vol. 15, no. 2, pp. 430–436, Jan. 2007.

[7] S. F. Preble, Q. Xu, and M. Lipson, "Changing the color of light in a silicon resonator," *Nature Photon.*, vol. 1, pp. 293–296, May 2007.

[8] L. Zhou, H. Chen, and A. W. Poon, "NRZ-to-PRZ format conversion using silicon second-order coupled-microring resonator-based notch filters," in *Proc. CLEO/QELS 2007*, Baltimore, MD, May 6–11, 2007.

[9] J. Slovak, C. Bornholdt, J. Kreissl, S. Bauer, M. Biletzke, M. Schlak, and B. Sartorius, "Bit rate and wavelength transparent all-optical clock recovery scheme for NRZ-coded PRBS signals," *IEEE Photon. Technol. Lett.*, vol. 18, pp. 844–846, Apr. 2006.

[10] H. J. Lee, H. G. Kim, J. Y. Choi, and H. K. Lee, "All-optical clock recovery from NRZ data with simple NRZ-to-PRZ converter based on self-phase modulation of semiconductor optical amplifier," *Electron. Lett.*, vol. 35, no. 12, pp. 989–990, Jun. 1999.

[11] Y. D. Jeong, H. J. Lee, H. Yoo, and Y. H. Won, "All-optical NRZ-to-PRZ converter at 10 Gb/s based on self-phase modulation of Fabry-Perot laser diode," *IEEE Photon. Technol. Lett.*, vol. 16, pp. 1179–1181, Apr. 2004.

[12] X. Li, C. Kim, and G. Li, "All-optical passive clock extraction of 40 Gbit/s NRZ data using narrow-band filtering," *Opt. Expr.*, vol. 12, no. 14, pp. 3196–3203, July 2004.

[13] G. Contestabile, A. D'Errico, M. Presi, and E. Ciaramella, "40-GHz all-optical clock extraction using a semiconductor-assisted Fabry-Perot filter," *IEEE Photon. Technol. Lett.*, vol. 16, pp. 2523–2525, May 2004.

[14] G. Contestabile, M. Presi, N. Calabretta, and E. Ciaramella, "All-optical clock recovery from 40 Gbit/s NRZ signal based on clock line enhancement and sharp periodic filtering," *Electron. Lett.*, vol. 40, no. 21, pp. 1361–1362, Oct. 2004.

[15] B. Franz, "Optical signal processing for very high speed (>40 Gbit/s) ETDM binary NRZ clock recovery," in *Proc. Opt. Fiber Commun. Conf.*, 2001, pp. MG1-1–MG1-6.

[16] C. Kim, I. Kim, X. Li, and G. Li, "All-optical clock recovery of NRZ data at 40 Gbit/s using Fabry-Perot filter and two-section gain-coupled DFB laser," *Electron. Lett.*, vol. 39, no. 20, pp. 1456–1457, Oct. 2003.

[17] H. K. Lee, C. H. Lee, S. B. Kang, M.-Y. Jeon, K. H. Kim, J. T. Ahn, and E.-H. Lee, "All-fibre-optic clock recovery from non-return-to-zero format data," *Electron. Lett.*, vol. 34, no. 5, pp. 478–480, Mar. 1998.

[18] W. W. Tang, M. P. Fok, and C. Chu, "All-optical clock recovery from NRZ data using a NRZ-to-PRZ converter constructed with a polarization-maintaining fiber loop mirror filter," in *Proc. Conf. Lasers Electro-Opt.*, 2005, pp. 1198–1199.

[19] C.-H. Lee and H. K. Lee, "Passive all-optical clock signal extractor for non-return-to-zero signals," *Electron. Lett.*, vol. 34, no. 3, pp. 295–297, Feb. 1998.

[20] J. Yu, G. K. Chang, J. Barry, and Y. Su, "40 Gbit/s signal format conversion from NRZ to RZ using a Mach-Zehnder delay interferometer," *Opt. Commun.*, vol. 248, no. 4–6, pp. 419–422, Apr. 2004.

[21] H. K. Lee, J. T. Ahn, M. Y. Jeon, K. H. Kim, D. S. Lim, and C.-H. Lee, "All-optical clock recovery from NRZ data of 10 Gb/s," *IEEE Photon. Technol. Lett.*, vol. 11, pp. 730–732, Jun. 1999.

[22] K. M. Ho, "Electroabsorption-modulator based clock recovery circuit for high-speed optical non-return-to-zero (NRZ) signals," M.Phil. thesis, Hong Kong Univ. Sci. Technol., Hong Kong, China, Jul. 2005.

[23] R. A. Soref and B. R. Bennett, "Electrooptical effects in silicon," *IEEE J. Quantum Electron.*, vol. QE-23, pp. 123–129, Jan. 1987.

[24] A. Yariv, "Universal relations for coupling of optical power between microresonators and dielectric waveguides," *Electron. Lett.*, vol. 36, no. 4, pp. 321–322, Feb. 2000.

[25] V. Nguyen, T. Montalbo, C. Manolatou, A. Agarwal, C. Y. Hong, J. Yasaitis, L. C. Kimerling, and J. Michel, "Silicon-based highly-efficient fiber-to-waveguide coupler for high index contrast systems," *Appl. Phys. Lett.*, vol. 88, Feb. 2006.

[26] V. R. Almeida, R. R. Panepucci, and M. Lipson, "Nanotaper for compact mode conversion," *Opt. Lett.*, vol. 28, no. 15, pp. 1302–1305, Aug. 2003.

[27] J. Niehusmann, A. Vörckel, and P. H. Bolivar, "Ultrahigh-quality-factor silicon-on-insulator microring resonator," *Opt. Lett.*, vol. 29, no. 24, pp. 2861–2863, Dec. 2004.

[28] M. S. Nawrocka, T. Liu, X. Wang, and R. R. Panepucci, "Tunable silicon microring resonator with wide free spectral range," *Appl. Phys. Lett.*, vol. 89, Aug. 2006.

[29] B. Maune, R. Lawson, C. Gunn, A. Scherer, and L. Dalton, "Electrically tunable ring resonators incorporating nematic liquid crystals as cladding layers," *Appl. Phys. Lett.*, vol. 83, no. 23, pp. 4689–4691, Dec. 2003.

Linjie Zhou received the B.S. degree in microelectronics from Peking University, Beijing, China, in 2003 and the Ph.D. degree in electronic and computer engineering at The Hong Kong University of Science and Technology, Hong Kong SAR, China, in 2007.

He is currently with the Department of Electrical and Computer Engineering, University of California at Davis.

Hui Chen (S'02) received the B.E. degree in telecommunication engineering from Beijing University of Posts and Telecommunications, Beijing, China, in 2000 and the M.Phil. degree in electrical and electronic engineering from The Hong Kong University of Science and Technology, Hong Kong SAR, China, in 2003, where he is currently pursuing the Ph.D. degree in electronic and computer engineering.

Andrew W. Poon (M'07) received the B.A. (Hons.) degree from the University of Chicago, Chicago, IL, and the M.Phil. and Ph.D. degrees from Yale University, New Haven, CT, in 1995, 1998, and 2001, respectively, all in physics.

He is currently an Associate Professor in the Department of Electronic and Computer Engineering, The Hong Kong University of Science and Technology, Hong Kong SAR, China. His current research interests include experiments and designs of novel optical microresonators and silicon-based photonic passive and active devices and circuits.